International Journal of Environment and Geoinformatics 10(1):001-008 (2023)

Research Article

Determination of Urban Areas Using Google Earth Engine and Spectral Indices; Esenyurt Case Study

Zelal Kaya[1], Adalet Dervisoglu [2,*]

[1] Graduate School, Informatics Institute, Geographical Information Technologies, Istanbul Technical University, Istanbul, TURKIYE
[2] Geomatics Engineering, Civil Engineering, Istanbul Technical University, Istanbul, TURKIYE

* Corresponding author: A. Dervisoglu
* E-mail: adervisoglu@itu.edu.tr

Received 03.08.2021
Accepted 22.12.2022

How to cite: Kaya and Dervisoglu(2023). Determination of Urban Areas Using Google Earth Engine and Spectral Indices; Esenyurt Case Study. *International Journal of Environment and Geoinformatics (IJEGEO)*, 10(1): 001-008. doi. 10.30897/ijegeo.1214001

Abstract

Identifying impervious surfaces for monitoring urban expansion is important for the sustainable management of land resources and the protection of the environment. Remote sensing provides an important data source for urban land use/land cover mapping and these data can be analyzed with various techniques for different purposes. If the aim is to extract information easily and rapidly, using spectral indices is the most appropriate solution, and many indices were created for this purpose. Esenyurt, which is the most populous district of Istanbul, was investigated by applying eight urban spectral indices and three vegetation indices to Sentinel 2 MSI image in the Google Earth Engine (GEE) platform. Accuracy assessments were made using the same points for all indices results. Since tile roofs and bare soil areas give similar reflectance values, they were more or less mixed, and the Band Ratio for the Built-up Area (BRBA) gave the best result in urban index applications; the overall accuracy is 91%. However, all three applied vegetation indices gave better results than the urban indices, and the Normalized Difference Vegetation Index (NDVI) gave the best result among all indices with an overall accuracy of 95 %. NDVI time series, which gives the highest accuracy, was applied to the entire area within the district borders in GEE using Landsat 5 and Landsat 8 images between 1990-2022. While the average NDVI values in May 1990 were 0.554 within the district's boundaries, it was determined as 0.22 in May 2022. A high negative correlation (-0.81) was determined between the NDVI mean values and the 1990-2022 population data. While the population growth in the district increased at a very high rate from 1990 to 2022 (1604%) (from 2008 to 2022, 302%), green areas rapidly disappeared due to the rapidly increasing population and rapid urbanization.

Keywords: Spectral Indices, BRBA, NDVI, GEE, Esenyurt

Introduction

Rapidly developing urbanization trend requires frequent updating of surface maps. Land use and land cover (LULC) maps are essential for city planning, environmental, and disaster management. Urbanization causes many adverse environmental effects, such as the conversion of natural areas to artificial surfaces, climate change, and a decrease in water quality. The relationship between urbanization and environmental impacts can be analyzed by mapping their dimensions and intensities in relation to urban expansion. Urban characteristics can be estimated and measured using several methods, including field measurements, visualization and interpretation of aerial photographs and satellite imagery, and digital interpretation of remote sensing (RS) data.

RS urban applications are now indispensable from planning to city management, and old maps and field surveys for city surveys are out of date and have been replaced by RS images rapidly (Netzband et al. 2007). Many urban land use mapping studies have been made with RS images and methods, from the global scale to the regional mapping of a single city (Duan et al. 2015; Trianni et al. 2015; Liu et al. 2018; Wang et al. 2017; Magidi and Ahmed, 2019; Misra et al. 2020, Zhang et al. 2021; Kebede et al.,2022).

The use of remotely sensed images depends on the purpose and detail of the studies. Especially for urban area studies, a high spatial resolution is needed to support detailed land use classification. Therefore, an image with high spatial resolution and diverse spectral characteristics become a good alternative for urban studies addressing an urban area's complexity and spatial heterogeneity (Hidayeti et al., 2018).

Various urban problems can be solved by classifying the images in different spatial resolutions according to usage purposes or surface coatings. For this purpose, classification methods or various indices are used. Many methods are developed and used for the classification of images in the literature, including supervised image classification, unsupervised methods, parametric classifiers, non-parametric classifiers, object-oriented classifiers, regression trees, support vector machines, artificial neural networks, etc. And also, many established indices have been proposed in the literature to classify urban areas as urban and non-urban areas (Javed et al. 2021). Urban spectral indices, generating LULC maps, forecasting, change detection, time series

analysis, urban dynamics, monitoring, modeling, etc., were used in operations and led to promising developments. Remote sensing spectral indices are unsupervised, unbiased, fast, scalable, and quantitative in information extraction (Javed et al. 2021).

Javed et al. (2021) summarized the urban spectral indices in the literature, they used the terms "urban index", "built-up index", "normalized difference built-up area", " impervious surface index", and "spectral urban index"; and the research was conducted in the "Web of Science Core" database. Urban indices using multi-spectral bands were separated according to the spectral wavelength range of the bands used. There are twenty-three indices in the tables listing the urban indices formed with bands in the spectral wavelength range of 400–2500 nm, except for panchromatic (PAN) bands. They identified three indices produced using PAN bands. The aim of the study is to investigate the applicability of urban, vegetation and soil spectral band indices in urban areas and to examine the temporal change of the district with the most appropriate indices. The indices were applied to the Sentinel 2 MSI image dated November 24, 2022. The most appropriate indices were determined for the extraction of urban areas; using this index, the Landsat time series was created for the area within the borders of the Esenyurt district in GEE. The change that occurred in thirty-two years was evaluated with the population data belonging to the same time range.

Study area

The population of Istanbul, which is the most populous city in Turkey, is 15.8 million according to 2021 data, and the population growth rate is 24.2‰ (Url-1). The most populous district of Turkey, with a population of 977 489 and an annual population growth rate of ‰ 20.8 (Url-1), is the Esenyurt district of Istanbul, which was chosen as the study area (Figure 1). In the past, the population of Esenyurt, which was a village dealing with agriculture, animal husbandry, and fisheries, increased rapidly due to the establishment of industrial facilities that started in the 1970s, cheap housing compared to the center and intense internal migration, and gained the status of a district in 2008.

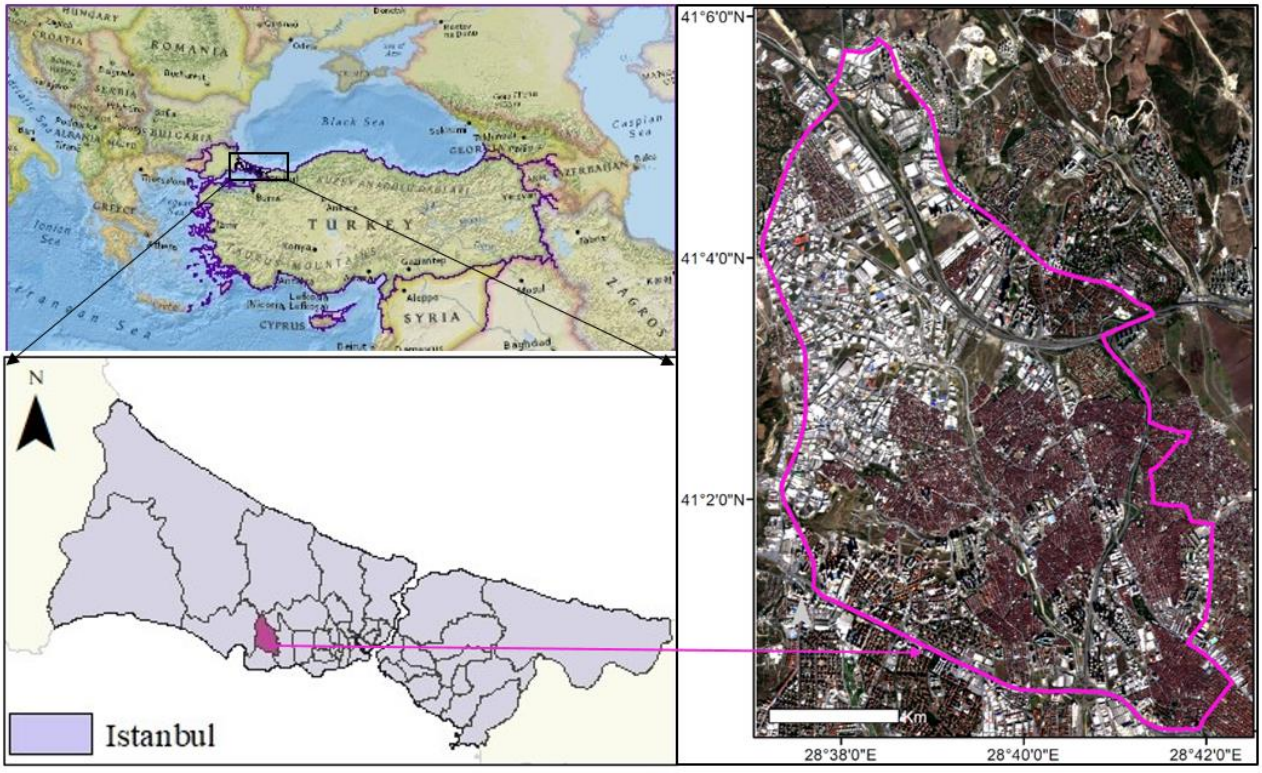

Fig. 1 Study Area (Esenyurt District).

Materials and Methods

In the study, Sentinel-2 MSI surface reflectance image dated 24 November 2022 was used to examine the indices. The urban and vegetation indices selected from the literature and used in the study are given in Table 1 with their formulas and references. The time series was generated with Landsat 5 TM and Landsat 8 OLI surface reflectance images. The characteristics of the satellite data used in the study were given in Table 2 (Url-2, Url-3, Url-4).

Google Earth Engine platform was used in the study. Earth Engine is a cloud platform for scientific analysis and visualization of geospatial datasets for users. Earth Engine hosts satellite imagery in a public data archive, including historical earth images dating back more than forty years. The images taken daily are then made available for data mining on a global scale. Earth Engine also provides APIs and other tools to analyze large data sets (Url-5).

Otsu's thresholding method corresponds to the linear discriminant criteria that assume that the image consists of only an object (foreground) and background; the background's heterogeneity and diversity are ignored

(Yousefi, 2011). The method processes image histograms, segmenting the objects by minimizing the variance in each class. Usually, this technique produces appropriate results for bimodal images. In GEE, threshold values were tried to be determined in indices by using the Otsu tresholding method (Otsu,1979), but it was seen that the method was not very successful in urban indices. The threshold values were determined by examining the images visually. Accuracy assessments were applied in GEE for eleven indices images created. The pixels in the thematic raster map were compared with the reference pixels created for each class the confusion matrices was generated, and overall accuracies, producer and user accuracies, and kappa accuracies were calculated (Çelik et al., 2022).

Table1. Indices used in the study.

Index Name	Index ID	Formula	Reference
Urban Index	UI	$(\frac{(SWIR2-NIR)}{(SWIR2+NIR)} + 1.0) * 100$	Kawamura et al. (1996)
Normalized Difference Tillage Index	NDTI	$\frac{-SWIR2)}{+SWIR2)}$	Van Deventer et al. (1997)
Normalized Difference Built-up Index	NDBI	$\frac{(SWIR1 - NIR)}{(SWIR1 + NIR)}$	Zha et al. (2003)
New built-up Index	NBI	$\frac{SWIR1 * RED}{NIR}$	Jieli et al. (2010)
Built-up Index	BUI	*NDBI- NDVI*	He et al. (2010)
Normalized Built-up Area Index	NBAI	$\frac{SWIR2 - (SWIR1/GREEN)}{SWIR2 + (SWIR1/GREEN}$	Waqar et al. (2012)
Band Ratio for the Built-up Area	BRBA	$\frac{RED}{SWIR1}$	Waqar et al. (2012)
Built-up area Extraction Index	BAEI	$\frac{(RED + 0.3)}{(GREEN + SWIR1)}$	Bouzekri et al. (2015)
Normalized Difference Vegetation Index	NDVI	*(NIR-RED)/(NIR+RED)*	Colwell (1974)
Soil Adjusted Vegetation Index	SAVI	$(1 + L) * \frac{(NIR - RED)}{(NIR + RED + L)}$ *L=0.5*	Huete (1988)
Enhanced Vegetation Index	EVI	$2.5 * \frac{NIR-RED}{NIR + 6 * RED - 7.5 * BLUE + 1.0}$	Url 6-7

Table 2. The characteristics of the satellite data used in the study.

Satellite	**Spectral ranges (µm)**	**Spatial Resolution (m)**	**Temporal Resolution (day)**	**Radiometric Resolution**
Sentinel-2 MSI	B1: 0.43-0.45, B2: 0.46-0.52, B3: 0.54-0.58, B4:0.65-0.68, B5: 0.70-0.71, B6:0.73-0.75 B7: 0.77-0.79, B8: 0.79-0.90 B8A: 0.86-0.88, B11:1.57-1.66, B12: 2.10–2.28	B2-4, B8: 10 m B5-7, B8A, B11-12: 20 m B1, B9: 60 m	5	12 bits
Landsat 5 TM	B1: 0.45-0.52, B2: 0.52-0.60 B3: 0.63-0.69, B4: 0.76-0.90 B5: 1.55-1.75, B6: 10.40-12.50, B7: 2.08-2.35	B1-B5, B5:30m B6:120 (30) m	16	8 bit
Landsat 8 OLI-TIRS	B1: 0.43-0.45, B2:0.45-0.51 B3: 0.53-0.59, B4: 0.64-0.67 B5: 0.85-0.88, B6:1.57-1.65 B7: 2.11-2.29, B8: 0.50-0.68 B9: 1.36-1.38, B10:10.60-11.19 B11: 11.50–12.51	B1-B7, B9:30m B8:15m B11,B12:100m	16	12 bit

Results

The images obtained as a result of the application of the indices are given in Figure 2. When the results of indices in the images in Figures 2 were examined, it was seen that urban areas were shown with a light color in some indexes and were shown with in dark tones in some indices.

The minimum and maximum values of the images and the pixel values of the urban areas were given in Table 3. Since the results of indices produced with urban indices are not bimodal, the correct threshold value could not be

calculated with Otsu's threshold method. For instance, the two related histograms were given in Figure 3.

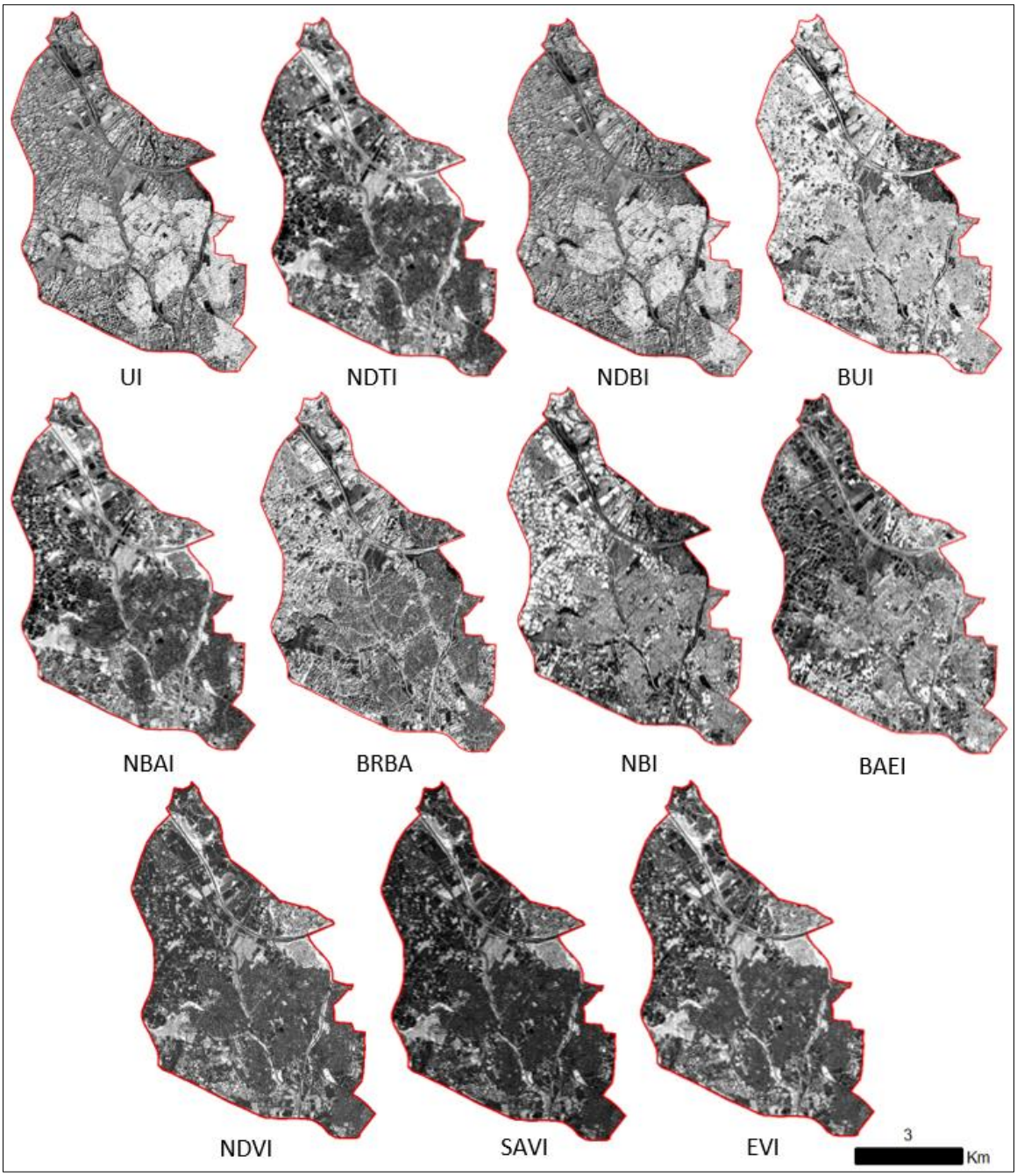

Fig. 2 Sentinel 2 image, and images obtained as a result of indices applications.

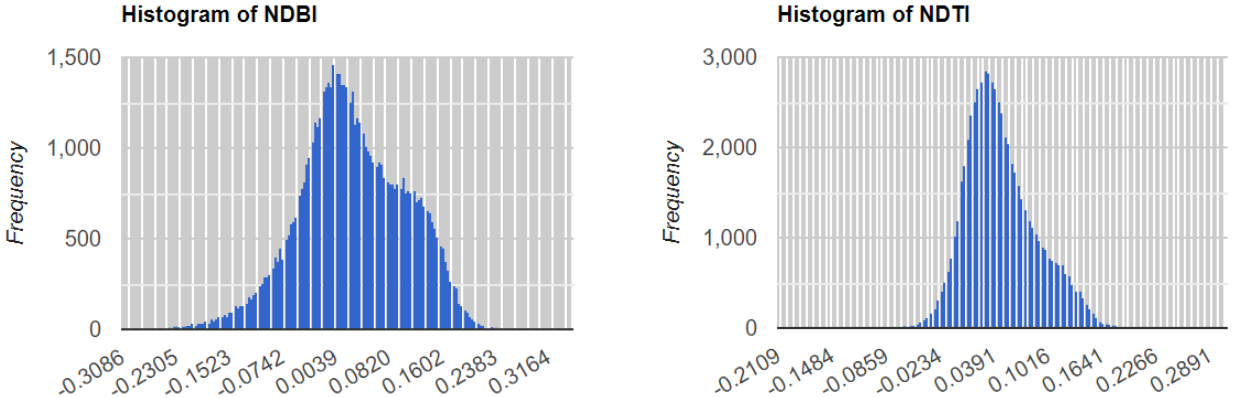

Fig. 3 NDBI and NDTI image histograms.

Urban and non-urban areas in the images were examined visually with pixel values. In all of the urban indices used, it was observed that land areas, especially bare soil and urban areas, were mixed. The BRBA outperformed all other indices in distinguishing bare soil and urban areas. The minimum and maximum values of the images and results are given in Table 3.

Table 3. Minimum, maximum values and ranges of Images.

Indices	min	max	Urban*~	Soil*~
NDBI	-0.304	0.3253	0.08-0.50	0.02-0.25
NBI	0.017	0.261	0.10-0.40	0.05-0.14
BRBA	0.188	1.051	0.50-0.90	0.20-0.60
NDTI	-0.035	0.268	≤ 0.15	0.11-0.20
BUI	-1.005	0.786	-0.30-0.35	-0.10-0.60
BAEI	0.908	2.330	0.91-1.80	1.00-1.60
UI	64.60	139.22	90-130	100-200
NBAI	-0.971	-0.637	-0.30-0.90	-0.70-0.95
NDVI	-0.030	0.850	-0.02-0.10	0.11-0.16
SAVI	-0.247	0.278	-0.01-0.04	0.01-0.20
EVI	11.5	255.5	40-120	60-155

**: These values were obtained from the analyzed pixels within the district's boundaries in the images.*

Binary images (urban and non-urban) were created using the threshold values for all indices application results. Then, using the same points (urban:50 non-urban:50) for each index results, the accuracy assessments were applied in GEE. The results of the accuracy assessment are given in Table 4 with overall accuracy (OA), and kappa statistics.

Table 4. Accuracy assessment.

Indices	OA(%)	Kappa
NDBI	71	0.50
NBI	86	0.68
BRBA	**91**	**0.84**
NDTI	88	0.74
BUI	72	0.58
BAEI	74	0.63
UI	50	0.42
NBAI	65	0.46
NDVI	**95**	**0.89**
SAVI	93	0.86
EVI	93	0.85

As a result of the accuracy assessment, the best result among the eleven indexes was obtained with NDVI, and a two-class image (urban, non-urban) was obtained by using the threshold value (0.3) for this index image. (Figure 4).

With the rapid urbanization in Esenyurt District, green areas were disappeared, and artificial surfaces were taken their places. To determine this change, NDVI was applied to the surface reflection images of Landsat 5 TM and Landsat 8 OLI on the GEE platform.

The NDVI average values of the green areas within the district boundaries were graphically obtained using the images acquired between 1990-2022 (cloud-free images covering all months, approximately 900 Landsat images). In Figure 5, the long-term change in the district was given by time series analysis.

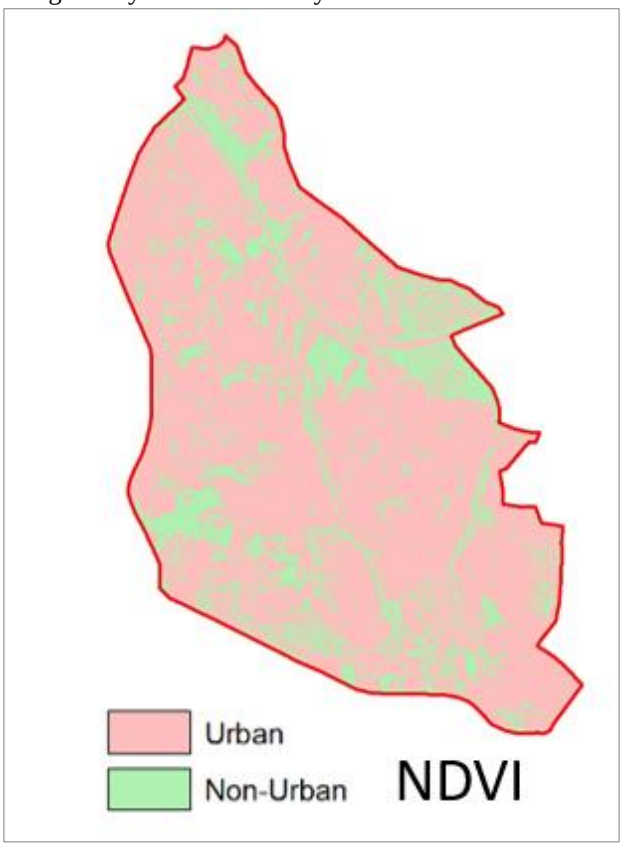

Fig. 4 Classified NDVI image.

The averages for May, when the vegetation is the most intense, were calculated from the graphic values covering all the months. A graph was created using the 32-year NDVI May value and district population data from TUIK, trends were determined, and the correlation of the data was examined (Figure 6).

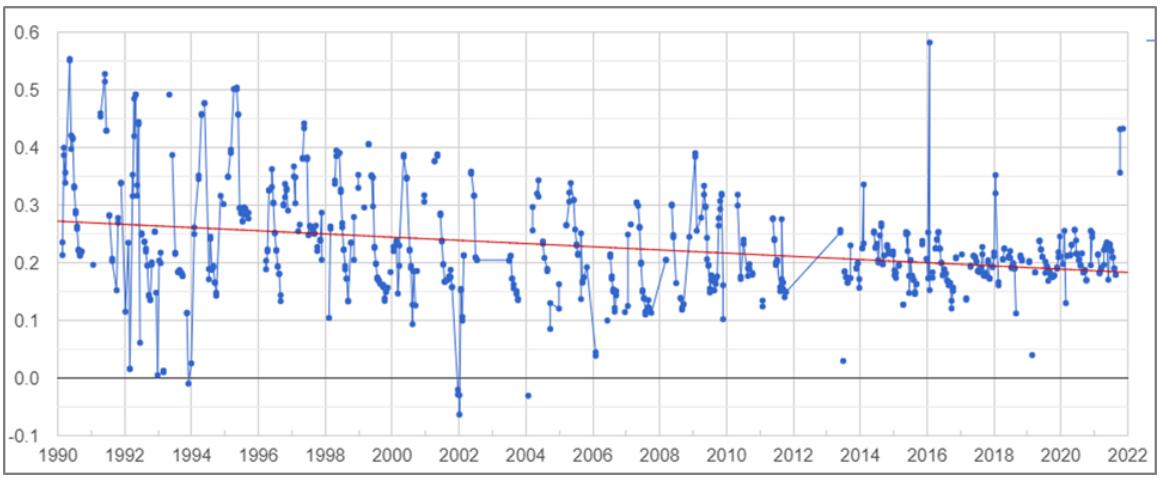

Fig. 5 Esenyurt district, 1990-2022 NDVI time-series (all months).

When the NDVI time series of the Esenyurt district given in Figure 5 are examined, a decreasing trend was observed in NDVI values from 1990 to 2022. NDVI values theoretically range from (–1) to (+1). In regions with dense green vegetation, the index value approaches +1, while cloud, water, and snow have low (minus) NDVI values. In the case of bare soil and poor vegetation, the NDVI value approaches zero (Colwell,1974). It was seen that the NDVI values were high in the series of the 1990s; that is, the vegetation is dense within the boundaries of the district. However, these values have decreased over time and decreased to 0.2 values, especially since 2010.

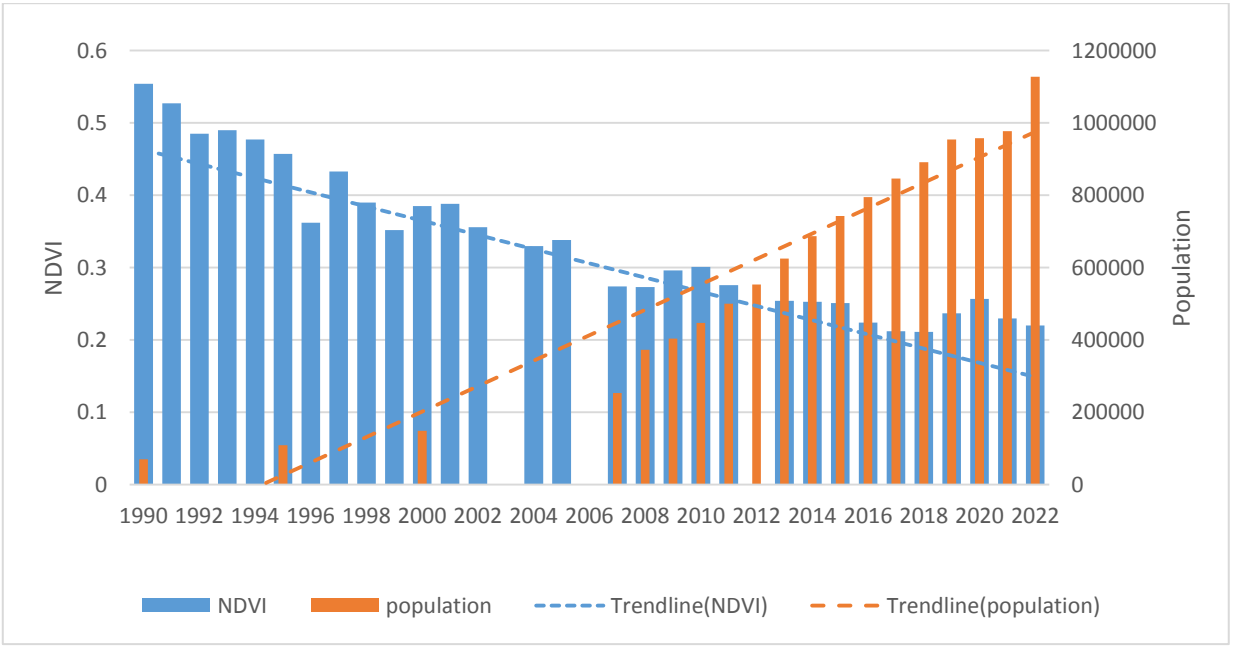

Fig. 6. NDVI values (May averages) and Esenyurt district population data.

The change in vegetation cover between 1990 and 2022 can be seen in Figure 7, using the average NDVI values of May, when the vegetation is most intense. The vegetation density has been decreasing rapidly since 1990, continued to decline since 2007, but the change was less. In the district where 70 thousand people lived in 1990, this number reached 148 thousand in 2000, 373 thousand in 2008 when it gained district status, and 977 thousand in 2021. According to the 2022 data of the address-based population registration system, Esenyurt, which is the largest district of Turkey in terms of population, with 1,127,489 people, has a population increase of 302 percent from 2008 to 2022. Considering the population values from 1990 to 2022, the population change is 1604%. As a result of the rapid increase in the population, it was seen in the graph that the green areas have been rapidly disappearing due to the increasing housing need in the district.

Discussion and Conclusion

Spectral indices are mathematical formulas created using two or more spectral bands in a multispectral image for easy and fast information extraction. Spectral indices are designed to highlight pixels in an image that indicate relative abundance or lack of land cover-type interest. Many indices produced for different land cover types are available in the literature. This study investigated the usability of city indices created to extract urban areas from Sentinel-2A satellite images. The main problem in

mapping urbanized areas is to separate bare land from impermeable surfaces and residential areas. BRBA was determined as the index that confusing tile roofs and soil areas at least. Three commonly used vegetation indices were applied to the same area, and better results were obtained in all three of them than the urban indices, and the best result was obtained with NDVI.

A rapid decrease in green areas was observed when NDVI time series was applied using Landsat 5 and Landsat 8 images to the entire area in GEE within the district boundaries for the years 1990-2022. There is a high negative correlation (-0.81) between the average NDVI mean values of the district in May and the 1990-2022 population data. The population within the district's boundaries has increased by 1604% from 1990 to 2022, rapid urbanization has occurred with the increasing population, and green areas have disappeared.

While urban index-based methods are quick and easy to implement, their ability to distinguish bare soil from urban areas is certainly challenging. This study showed that the built land class could not be determined efficiently using an index produced from multispectral bands alone, as in other studies with urban indices. When different studies using city indices are examined in the literature, the index that gives the best results changes, and a consensus cannot be reached on a single index. In addition, it has been observed that the structure of the indexed area and the selected threshold value affect the accuracy of the index used.

The high accuracies obtained in the evaluation made with indexes in the study can also be associated with the fact that a large part of the study area is covered with artificial surfaces. Although index-based methods are fast and easy to implement, they can only be used to form a general idea; they cannot replace classification methods.

Acknowledgements

The research presented in this article was created from the first author's master's thesis at Istanbul Technical University Informatics Institute.

References

Bouzekri, S., Lasbet, A. A., Lachehab, A. (2015). A new spectral index for extraction of built-up area using Landsat-8 data. *Journal of the Indian Society of Remote Sensing*, 43(4), 867-873.

Colwell, J. E. (1974). Vegetation canopy reflectance. *Remote Sensing Environment*, 3(3), 175-183.

Çelik, O. İ., Çelik, S., Gazioğlu, C. (2022). Evaluation on 2002-2021 CHL-A Concentrations in the Sea of Marmara with GEE Enhancement of Satellite Data, *International Journal of Environment and Geoinformatics*, 9(4), 68-77. doi.10.30897/ijegeo.1066168

Das, S., Angadi, D. P. (2022). Land use land cover change detection and monitoring of urban growth using remote sensing and GIS techniques: A micro-level study. *GeoJournal*, 87(3), 2101-2123.

Duan, Y., X. Shao, Y. Shi, H. Miyazaki, K. Iwao, R. Shibasaki.(2015). Unsupervised global urban area mapping via automatic labeling from ASTER and PALSAR satellite images. *Remote Sensing* 7(2):2171–2192.

He, C., Shi, P., Xie, D., Zhao, Y. (2010). Improving the normalized difference built-up index to map urban built-up areas using a semiautomatic segmentation approach. *Remote Sensing Letters*, 1(4), 213-221.

Hidayati, I. N., Suharyadi, R., Danoedoro, P. (2018). Exploring spectral index band and vegetation indices for estimating vegetation area. *Indonesian Journal of Geography*, *50*(2), 211-221.

Huete, A. R. (1988). A soil-adjusted vegetation index (SAVI). *Remote Sensing of Environmen*t, 25(3), 295-309.

Javed, A., Cheng, Q., Peng, H., Altan, O., Li, Y., Ara, I., ... & Saleem, N. (2021*).* Review of Spectral Indices for Urban Remote Sensing. *Photogrammetric Engineering & Remote Sensing*, 87(7), 513-524.

Jieli, C., Manchun, L. I., Yongxue, L. I. U., Chenglei, S., Wei, H. U. (2010). Extract residential areas automatically by new built-up index. In 2010 *18th International Conference on Geoinformatics* (pp. 1-5). IEEE.

Kawamura, M. Jayamana. S., Tsujiko, Y. (1996). Relation between social and environmental conditions in Colombo Sri Lanka and the urban index estimated by satellite remote sensing data. *Int. Arch. Photogramm. Remote Sens*, 31, 321-326.

Kebede, T. A., Hailu, B. T., Suryabhagavan, K. V. (2022). Evaluation of spectral built-up indices for impervious surface extraction using Sentinel-2A MSI imageries: A case of Addis Ababa city, Ethiopia. *Environmental Challenges*, 8, 100568.

Liu, X., G. Hu, Y. Chen, X. Li, X. Xu, S. Li, F. Pei, S. Wang. (2018). High-resolution multi-temporal mapping of global urban land using Landsat images based on the Google Earth engine platform. *Remote Sensing of Environment*, 209:227–239.

Magidi, J., Ahmed, F. (2019). Assessing urban sprawl using remote sensing and landscape metrics: A case study of City of Tshwane, South Africa (1984–2015). *The Egyptian Journal of Remote Sensing and Space Science*, 22(3), 335-346.

Misra, M., Kumar, D., Shekhar, S. (2020). Assessing machine learning based supervised classifiers for built-up impervious surface area extraction from sentinel-2 images. *Urban Forestry & Urban Greening*, 53, 126714.

Netzband, M., W. L. Stefanov, C. Redman. (2007). *Applied Remote Sensing for Urban Planning, Governance and Sustainability.* Springer.

Otsu, N. (1979) A Threshold Selection Method from Gray-Level Histograms. *IEEE Transactions on Systems, Man, and Cybernetics*, vol. 9, no. 1, pp. 62-66, Jan. 1979, doi: 10.1109/TSMC.1979.4310076.

Trianni, G., Lisini, G., Angiuli, E., Moreno, E. A., Dondi, P., Gaggia, A., Gamba, P. (2015). Scaling up to national/regional urban extent mapping using Landsat data. *IEEE Journal of Selected Topics in*

Applied Earth Observations and Remote Sensing, *8*(7), 3710-3719.

Url-1:https://data.tuik.gov.tr/Search/Search?text=n%C3%Bcfus

Url-2: https://sentinels.copernicus.eu/web/sentinel/user -guides/sentinel-2-msi

Url-3: https://www.usgs.gov/landsat-missions/landsat-5

Url-4: https://www.usgs.gov/landsat-missions/landsat-8

Url-5: https://earthengine.google.com/faq/

Url-6: https://www.usgs.gov/landsat-missions/landsat-enhanced-vegetation-index

Url-7: https://custom-scripts.sentinel-hub.com/custom-scripts/sentinel-2/evi/#

Van Deventer, A. P., Ward, A. D., Gowda, P. H., Lyon, J. G. (1997). Using thematic mapper data to identify contrasting soil plains and tillage practices. *Photogrammetric engineering and remote sensing*, 63, 87-93.

Wang, R., Wan, B., Guo, Q., Hu, M., Zhou, S. (2017). Mapping regional urban extent using NPP-VIIRS DNB and MODIS NDVI data. *Remote Sensing*, 9(8), 862.

Waqar, M. M., Mirza, J. F., Mumtaz, R., Hussain, E. (2012). Development of new indices for extraction of built-up area & bare soil from landsat data. *Open Access Sci. Rep*, 1(1), 4.

Yousefi, J. (2011). Image binarization using otsu thresholding algorithm. *Ontario, Canada: University of Guelph*.

Zha, Y., Gao, J., Ni, S. (2003). Use of normalized difference built-up index in automatically mapping urban areas from TM imagery. *International journal of remote sensing*, 24(3), 583-594.

Zhang, Z., Wei, M., Pu, D., He, G., Wang, G., Long, T. (2021). Assessment of annual composite images obtained by Google Earth engine for urban areas mapping using random forest. *Remote Sensing*, 13(4), 748.